

MILLIMETER WAVE MICROSTRIP MIXER BASED ON GRAPHENE

G. Hotopan^{1,*}, S. Ver Hoeye¹, C. Vazquez¹, R. Camblor¹,
M. Fernández¹, F. Las Heras¹, P. Álvarez², and R. Menéndez²

¹Area of Signal Theory and Communications, Department of Electrical Engineering, University of Oviedo, Campus de Viesques, Edificio Polivalente s/n, mod. 8, 1a planta E-33203, Gijón, Spain

²Consejo Superior de Investigaciones Científicas, C/Francisco Pintado Fe, 26, E-33011, Oviedo, Spain

Abstract—In this work, a millimeter wave microstrip frequency-mixer design based on graphene is presented. The desired frequency mixing behavior is obtained using a nonlinear component consisting in a microstrip line gap covered by a graphene layer. The circuit includes microstrip filters that have been designed to obtain a high isolation between the input and output ports. The nonlinear behavior of the frequency mixer has been experimentally evaluated in the 38.6–40 GHz input signal frequency range, for different values of the input power and local oscillator power.

1. INTRODUCTION

Due to the flourishing development of nowadays technology as well as the saturation in the microwave spectrum, service providers and system designers are beginning to implement and design circuits at higher frequencies, one common election being the millimeter and the submillimeter wave bands. Besides the less congested spectrum, the advantages of the millimeter wave band, such as higher rate data transmissions, very efficient spectrum utilization, increased security of communication transmissions and size reduction, are vital characteristics for many military and civilian related applications [1–4].

The design of modern millimeter wave communication systems requires low cost and high performance frequency mixer modules.

Received 17 May 2011, Accepted 17 June 2011, Scheduled 23 June 2011

* Corresponding author: George Roberto Hotopan (ghotopan@tsc.uniovi.es).

Mixer based circuits, either in microstrip [5,6] or monolithic technology [7–9], typically use diodes [10–12] or transistors [13–15] as active components, in order to generate the nonlinear behaviour. Creating wideband mixers in microstrip technology can be a real challenge for many designers. Wideband mixers at millimeter wave frequencies have been presented using waveguide [16], suspended stripline [17] or finline configurations [18] with the RF signal directly coupled to the mixer diodes.

The present work focuses on implementing graphene as the nonlinear element that will enable the frequency mixing operation in the millimeter wave band. The very large carrier mobility ($\cong 200.000 \text{ cm}^2\text{V}^{-1}\text{s}^{-1}$ around 300 K if extrinsic disorder is eliminated) of graphene, being at least one order of magnitude greater than in Si and GaAs [19], makes it an interesting material for high frequency applications. Theory on the nonlinear electromagnetic behavior of graphene has been presented in [20, 21], where it is demonstrated that frequency multiplication effects as well as frequency mixing effects can be found up to terahertz frequencies.

In order to evaluate the nonlinear performance of this material, a microstrip frequency mixer is designed operating as a frequency downconverter from the millimeter wave band ($f_{RF} = 39.3 \text{ GHz}$, $f_{LO} = 36 \text{ GHz}$) to the microwave band ($f_{IF} = 3.3 \text{ GHz}$). Section 2 describes the proposed topology for the graphene based frequency mixer, while Section 3 presents the design, optimization and measurement results of the microstrip filter prototypes. In Section 4 the nonlinear behaviour of graphene is illustrated through various power sweeps of the input signals.

2. FREQUENCY MIXER TOPOLOGY

The topology of the graphene based frequency mixer circuit is shown in Fig. 1. The circuit is designed for the realization of a frequency downconversion of the input signals with central frequency at 39.3 GHz to the intermediate frequency band, centered at 3.3 GHz, through mixing with a 36 GHz local oscillator signal. The used nonlinear frequency mixing component consists in a microstrip line with a small gap covered by a few layer graphene film exfoliated from highly oriented pyrolytic graphite. The input signal and the local oscillator signal are provided to the nonlinear graphene based mixing component through bandpass filters centered at 39.3 GHz and 36 GHz respectively, ensuring a good isolation between the input ports. The downconverted signal is delivered to the output port through a wideband low-pass filter.

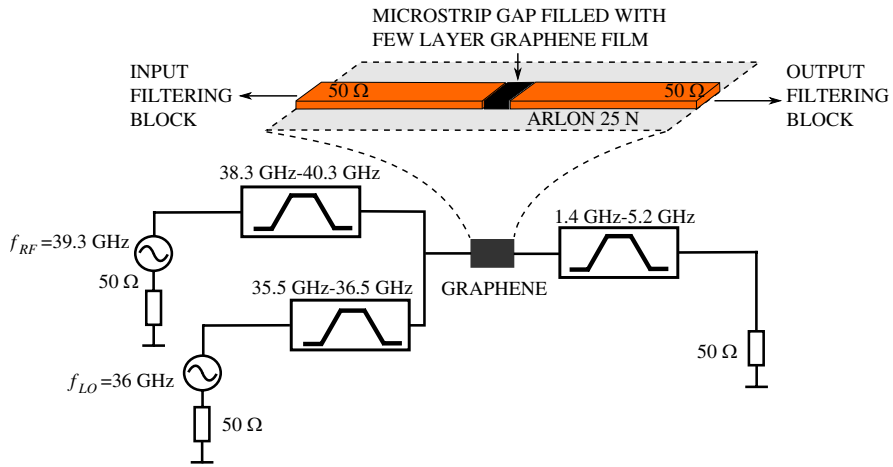


Figure 1. Topology of the millimeter wave frequency mixer.

3. FILTER DESIGN

All filters have been designed in an electromagnetic simulator (Method of Moments — MoM) using the same substrate (0.236 mm thick ARLON 25 N, $\epsilon_r = 3.38$, $\tan \delta = 0.0025$ at 10 GHz) that was employed for the implementation of the graphene based frequency mixing component.

The millimeter wave band-pass filters for the input and the local oscillator signals have been implemented using microstrip parallel coupled line configurations composed of six quarter-wavelength line resonators (Figs. 3(a), (b)). The filters have been designed to have a minimum 1.5 GHz bandwidth (for f_{RF}), respectively 1 GHz (for f_{LO}), and to ensure sufficient isolation between the input ports.

In order to combine the two injected signals, a microstrip diplexer was designed. The parametrized geometry of the diplexer was optimized using the ADS schematic simulator. Note that, during the optimization process a degree of freedom was left to the geometrical dimensions of the filters, some of the values suffering minor changes. The diplexer was designed to add minimum insertion losses in the frequency range containing the passbands of the two filters.

For the implementation of the low-pass output filter, an Arbitrarily Width Modulated Microstrip Line (AWMML) is employed [22]. The AWMML based filter is formed by a large number N of tapered microstrip sections of length $\Delta L = L_{AWMML}/N$. To avoid rough transitions between adjacent sections, the width modulating function is

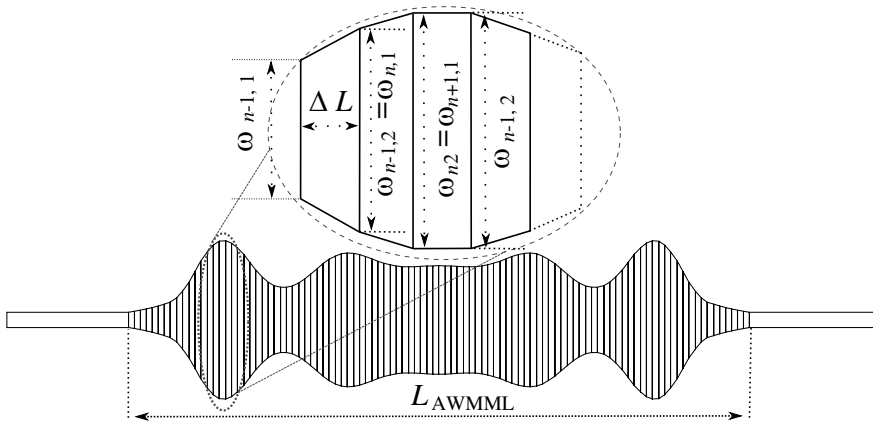


Figure 2. Topology of the AWMML filter.

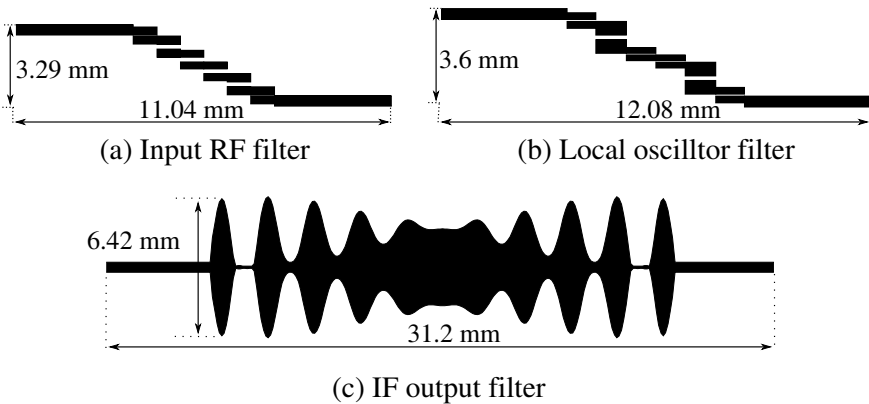


Figure 3. Layout of the fabricated filters.

chosen to be continuous, in such a way that the begin width $w_{n,1}$ of a specific section is equal to the end width $w_{n-1,2}$ of the previous section, as illustrated in Fig. 2.

During the optimization process, realized in a schematic simulator, the begin and end width of each section are varied. The total number of tapered microstrip sections used is $N = 200$. The total length of the AWMML filter is optimized by varying ΔL . Once the goals are satisfied, the layout of the filter can be created and simulated using the ADS MoM electromagnetic simulator. The layout of the optimized AWMML filter is shown in Fig. 3(c).

The performance of the circuit regarding the frequency selectivity as well as the isolation between the input ports has been evaluated using ADS MoM electromagnetic simulator. In order to validate the filter designs, two prototypes have been manufactured, a first circuit containing all elements of the mixer from the input ports to the microstrip line on the left side of the gap (Fig. 4(a)), and a second circuit containing the elements from the right side of the gap to the output port (Fig. 4(b)).

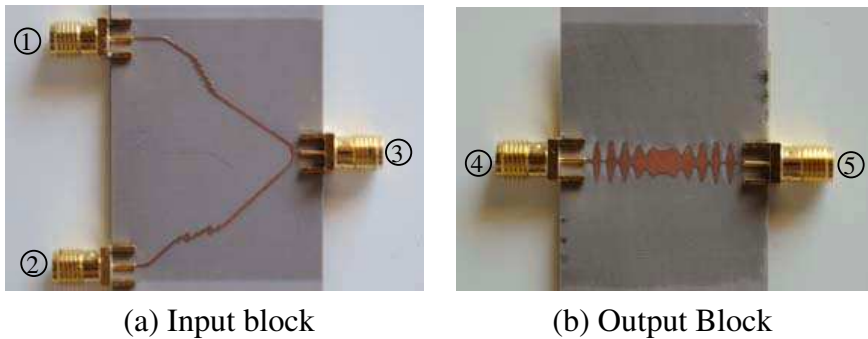
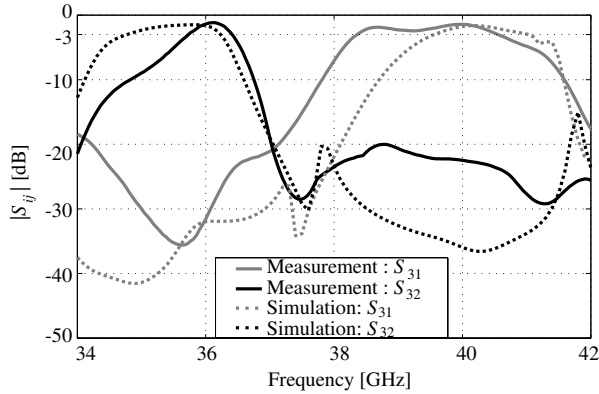


Figure 4. Fabricated filter prototypes.

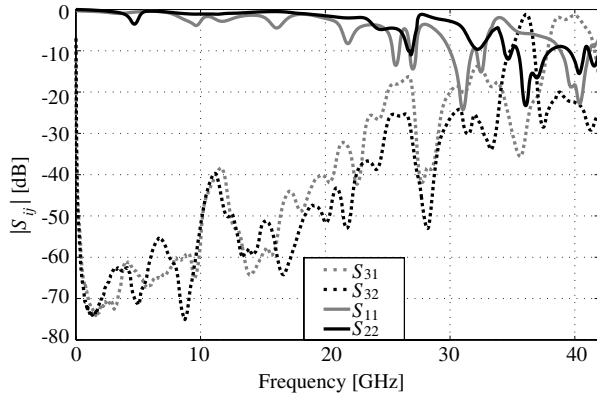
The measurement and simulation results are illustrated in Fig. 5 and Fig. 6. The performance of the filters was evaluated by measuring individually the S parameters of the two circuits. It can be seen that the input band-pass filters show a low insertion loss ($S_{31} = -2$ dB and $S_{32} = -2$ dB) at their corresponding central frequency and provide an isolation between the input ports higher than +20 dB. The measurements reveal that the first band-pass filter (BPF_1) has the central frequency $f_{c1} = 39.3$ GHz with a 5% fractional bandwidth, while for the second one (BPF_2), a $f_{c2} = 36$ GHz central frequency and a 2.7% fractional bandwidth have been obtained.

The measurements of the AWMML based filter (Fig. 6) show a central frequency $f_{c3} = 3.3$ GHz, with minimum insertion losses reaching values of +1 dB and a fractional bandwidth of 115%.

Slight differences are found in the frequency response of the filters due to inherent tolerances of the used manufacturing process for the microstrip designs, and to variations of ϵ_r at the operation frequency with respect to the value given by the provider (measured at 10 GHz).



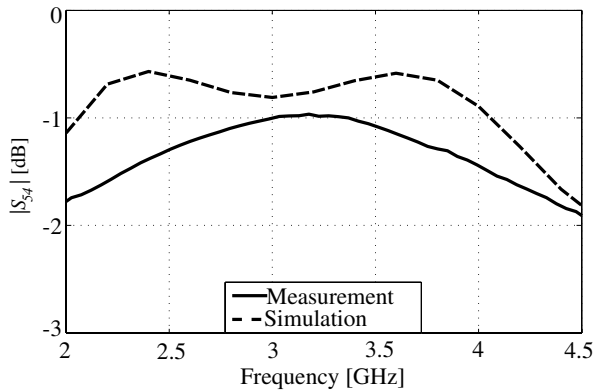
(a) Transmission coefficient: passband

(b) S parameters: measurements**Figure 5.** Measurement vs simulation of the band-pass filters.

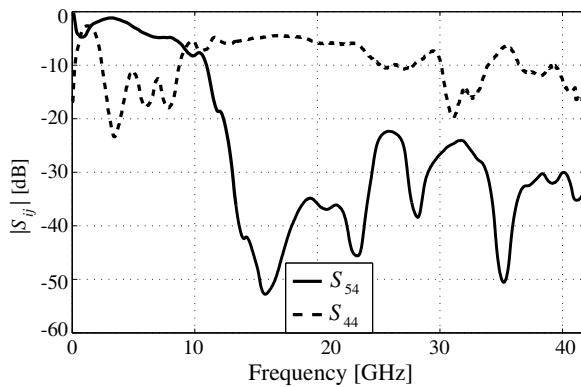
4. BEHAVIOR OF THE GRAPHENE BASED FREQUENCY MIXER

For the evaluation of the behavior of the graphene based frequency mixer, a prototype of the complete microstrip circuit was manufactured with a gap in the $50\ \Omega$ microstrip line that connects the diplexer with the output filter. The graphene based nonlinear mixing component has been completed by covering the gap with a few layer graphene film, exfoliated from a highly oriented pyrolytic graphite. A photo of the entire graphene based frequency mixer is presented in Fig. 8.

The mixer presents high LO, RF and IF port-to-port isolation with overall values better than 37 dB (LO/IF \geq 41 dB, LO/RF \geq 41 dB and



(a) Transmission coefficient: passband



(b) S parameters: measurements

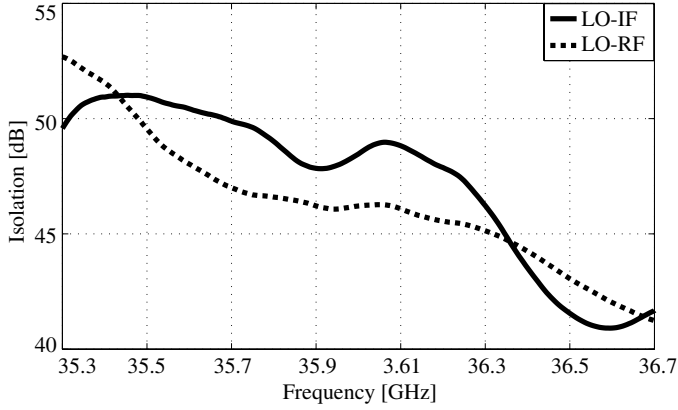
Figure 6. Measurement vs simulation of the AWMMML filter.

Table 1. Performance of the graphene based frequency mixer.

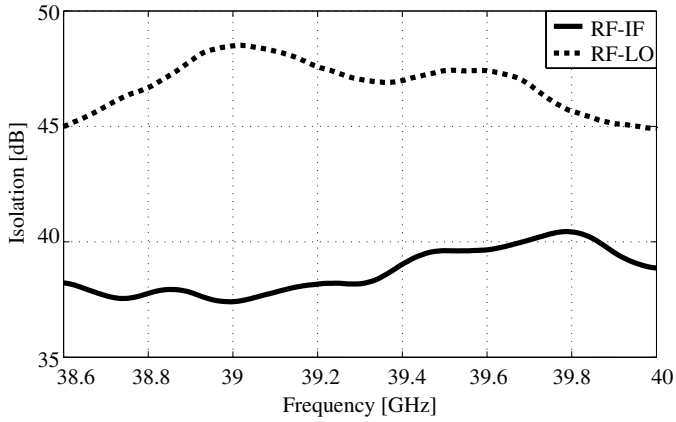
Isolation [dB]			P_{out} [dBm]		BW [GHz]		
LO/IF	LO/RF	RF/IF	$P_{in} \nearrow$	$P_{LO} \nearrow$	RF	LO	IF
≥ 41	≥ 41	≥ 37	-29	-31	1.5	1	1.4

RF/IF ≥ 37 dB), as depicted from Fig. 7.

The mixing behavior of the circuit has been evaluated, varying the frequency of input signal from 38.6 GHz to 40 GHz and for a constant 36 GHz local oscillator frequency, at different power values of the input signal $-10 \text{ dBm} \leq P_{in} \leq 10 \text{ dBm}$ and of the local oscillator signal $-5 \text{ dBm} \leq P_{LO} \leq 15 \text{ dBm}$. An evaluation of the output power levels P_{out} for a single frequency point ($f_{in} = 39.3 \text{ GHz}$) was also



(a)



(b)

Figure 7. Port-to-port isolation.**Table 2.** Comparison with other works found in the state-of-the-art.

	THIS WORK	[23]	[24]
Type	few layer graphene film	GFET	GFET
f_{RF}	39.3 GHz	3.8 GHz	10.5 MHz
f_{IF}	3.3 GHz	0.2 GHz	0.5 MHz
RF/IF BW	1.4 GHz	N.S.	N.S.
CL	40 dB	27 dB	30–40 dB

conducted, when varying the power levels of both injected signals. The measurement results are shown in Fig. 9. It can be observed that the efficiency in the frequency mixing operation obtained with the graphene based nonlinear component is almost frequency independent, being the variation of the output power mainly due to the frequency response of the used filters. For higher power values of the input signal and the local oscillator signal a slight saturation effect can be observed.

A summary containing the overall performance of the proposed millimeter wave frequency mixer based on graphene is presented in Table 1, while Table 2 shows a comparison between this work and others found in the state-of-the-art, where: CL — conversion loss; N.S — not specified; Type — refers to the type of the nonlinear element used.

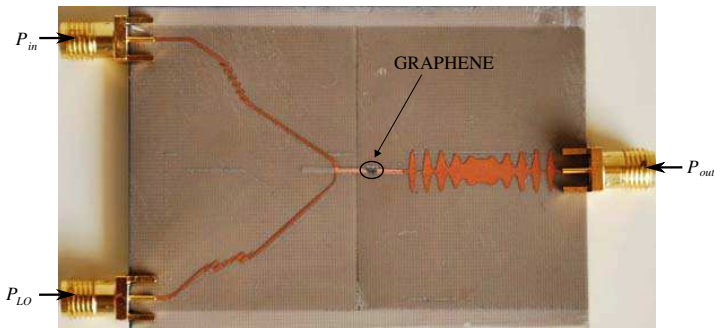
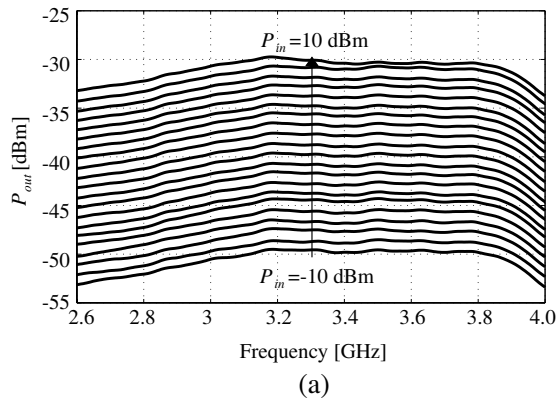
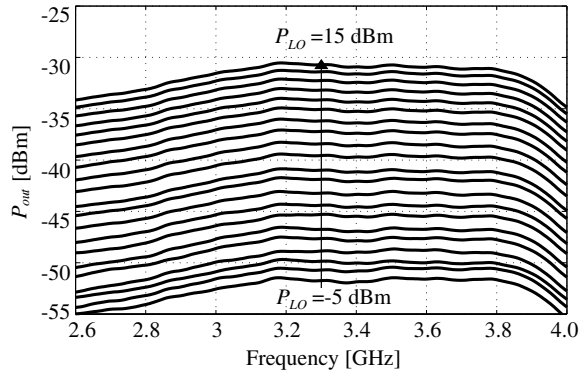
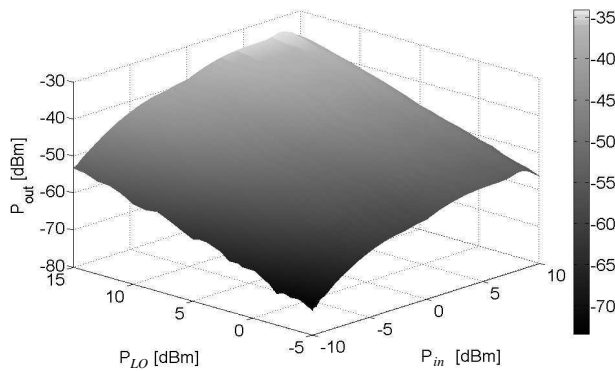


Figure 8. Manufactured prototype of the graphene based frequency mixer.





(b)



(c)

Figure 9. Relation between the provided input powers P_{in} and P_{LO} , and the measured output power P_{out} . (a) Measured output power P_{out} when varying P_{in} . (b) Measured output power P_{out} when varying P_{LO} . (c) 3D representation of output power at 3.3 GHz when varying both P_{in} and P_{LO} .

5. CONCLUSIONS

The nonlinear behavior of graphene layers has been demonstrated through the implementation of a nonlinear component consisting in a microstrip gap covered with a few layer graphene film exfoliated from a highly oriented pyrolytic graphite. The graphene based nonlinear component has been successfully integrated in a millimeter wave frequency mixer design implemented in microstrip technology. The obtained experimental results show a very flat frequency response

of the frequency mixing behavior over the whole input frequency band. A slight saturation of the output power has been observed at high power values of the input signal and local oscillator signal.

ACKNOWLEDGMENT

This work has been supported by the “Ministerio de Ciencia e Innovación of Spain /FEDER” under projects TEC2008-01638/TEC, CONSOLIDER-INGENIO CSD2008-00068 and grant AP2009-0438, by the “Gobierno del Principado de Asturias (PCTI)/FEDER-FSE” under projects EQUIP08-06, FC09-COF09-12, EQUIP10-31 and PC10-06, grant BP10-031 and by “Cátedra Telefónica - Universidad de Oviedo”.

REFERENCES

1. Hung, C.-Y., M.-H. Weng, R.-Y. Yang, and H.-W. Wu, “Design of a compact CMOS bandpass filter for passive millimeter-wave imaging system application,” *Journal of Electromagnetic Waves and Applications*, Vol. 23, No. 17–18, 2323–2330, 2009.
2. Yang, X.-D., Y.-S. Li, and C.-Y. Liu, “A toothbrush-shaped patch antenna for millimeter-wave communication,” *Journal of Electromagnetic Waves and Applications*, Vol. 23, No. 1, 31–37, 2009.
3. Gu, J., Y. Fan, Y.-H. Zhang, and D.-K. Wu, “A novel 3-D half-mode SICC resonator for microwave and millimeter-wave applications,” *Journal of Electromagnetic Waves and Applications*, Vol. 23, No. 11–12, 1429–1439, 2009.
4. Shireen, R., S. Shi, and D.-W. Prather, “Wideband millimeter-wave bow-tie antenna,” *Journal of Electromagnetic Waves and Applications*, Vol. 23, No. 5–6, 737–746, 2009.
5. Tahim, R.-S., T. Pham, and K. Chang, “Millimeter-wave microstrip subharmonically pumped mixer,” *IEEE Electronics Letters*, Vol. 21, No. 19, 861–862, September 1985.
6. Zhao, M., X. Zu, and J. Huang, “Low cost microstrip subharmonic mixer in millimeter wave band,” *International Conference on Microwave and Millimeter Wave Technology*, Builin, April 18–21, 2007.
7. Kawakami, K., M. Shimosawa, H. Ikematsu, K. Itoh, Y. Isota, and O. Ishida, “A millimeter-wave broadband monolithic even harmonic image rejection mixer,” *IEEE MTT-S Symp. Dig.*, 1443–1446, Baltimore, MA, June 7–12, 1998.

8. Lin, C.-M., J.-T. Chang, C.-C. Su, S.-H. Hung, and Y.-H. Wang, "A 16–31 GHz miniature quadruple subharmonic monolithic mixer with lumped diplexer," *Progress In Electromagnetics Research Letters*, Vol. 11, 21–30, 2009.
9. Lin, C.-M., Y.-C. Lee, S.-H. Hung, and Y.-H. Wang, "A 28–40 GHz doubly balanced monolithic passive mixer with a compact IF extraction," *Progress In Electromagnetics Research Letters*, Vol. 19, 171–178, 2010.
10. Hung, S.-H., W.-C. Chien, C.-M. Lin, Y.-A. Lai, and Y.-H. Wang, "V-band high isolation sub-harmonic monolithic mixer with hairpin diplexer," *Progress In Electromagnetics Research Letters*, Vol. 16, 161–169, 2010.
11. Zhang, B., Y. Fan, Z. Chen, X. F Yang, and F. Q. Zhong, "An improved 110-130-GHz fix-tuned subharmonic mixer with compact microstrip resonant cell structure," *Journal of Electromagnetic Waves and Applications*, Vol. 25, No. 2–3, 411–420, Feb. 2011.
12. Blackwell, D., H.-G. Henry, J.-E. Degenford, and M. Cohn, "94-GHz subharmonically pumped MMIC mixer," *IEEE MTT-S Symp. Dig.*, 1037–1039, Boston, MA, June 10–14, 1991.
13. Lai, Y.-A., S.-H. Hung, C.-N. Chen, and Y.-H. Wang, "A miniature millimeter-wave monolithic star mixer with simple IF extraction circuit," *Journal of Electromagnetic Waves and Applications*, Vol. 23, No. 17–18, 2433–2440, 2009.
14. Zirath, H., I. Angelov, N. Rorsman, and C. Karlsson, "A W-band subharmonically pumped resistive mixer based on pseudomorphic heterostructure field effect transistor technology," *IEEE MTT-S Symp. Dig.*, 341–344, Atlanta, GA, June 14–18, 1993.
15. Trotta, S., B. Dehlink, H. Knapp, K. Aufinger, T.-F. Meister, J. Bock, W. Simburger, and A.-L. Scholtz, "Design considerations for low-noise, highly-linear millimeter-wave mixers in SiGe bipolar technology," *33rd European Solid State Circuits Conference, ESSCIRC*, 356–359, Munich, September 11–13, 2007.
16. Raman, S., F. Rucky, and G.-M. Rebeiz, "A high-performance W-band uniplanar subharmonic mixer," *IEEE Transactions on Microwave Theory and Techniques*, Vol. 45, No. 6, 955–962, 1997.
17. Xie, J., "Suspended stripline and Ka band integrated mixer," *Asia-Pacific Conference on Environmental Electromagnetics*, Vol. 45, No. 6, 57–60, Shanghai, May 3–7, 2000.
18. Fu, J.-S., C.-Y. Yeh, H.-C. Chiu, K.-S. Chin, H.-L. Kao, and J.-C. Cheng, "Suspended substrate stripline (SSS) transition for high Q LO injected finline mixer," *Asia Pacific Microwave Conference, APMC*, Vol. 45, No. 6, 1–5, Macau, December 16–20, 2008.

19. Morozov, S.-V., K.-S. Novoselov, M.-I. Katsnelson, F. Schedin, D.-C. Elias, J.-A. Jaszczak, and A.-K. Geim, "Giant intrinsic carrier mobilities in graphene and its bilayer," *Physical Review Letters*, Vol. 100, January, 2008.
20. Mikhailov, S.-A. and K. Ziegler, "Nonlinear electromagnetic response of graphene: Frequency multiplication and the self-consistent-field effects," *Journal of Physics: Condensed Matter*, Vol. 20, 384204, 2008.
21. Mikhailov, S.-A., "Electromagnetic response of electrons in graphene: Non-linear effects," *Physica*, Vol. 40, 2626–2629, 2008.
22. Ver Hoeye, S., C. Vazquez Antuna, M. Gonzalez Corredoiras, M. Fernandez Garcia, L. F. Herran Ontanon, and F. Las Heras Andrés, "Multi-harmonic DC-bias network based on arbitrarily width modulated microstrip line," *Progress In Electromagnetics Research Letters*, Vol. 11, 119–128, 2009.
23. Lin, Y. M., A. Valdez-Garcia, S. J. Han, D. B. Farmer, I. Meric, Y. Sun, Y. Wu, C. Dimitrakopoulos, A. Grill, P. Avouris, and K. A. Jenkins, "Wafer-scale graphene integrated circuit," *Science*, Vol. 332, No. 6035, 1294–1297, June 10, 2011.
24. Wang, H., A. Hsu, J. Wu, J. Kong, and T. Palacios, "Graphene-based ambipolar RF mixers," *IEEE Electron Device Letters*, Vol. 31, No. 9, 906–908, 2010.